Predicting tensile strength of spliced and non-spliced steel bars using machine learning- and regression-based methods

Dabiri, Hamed; Kheyrodin, Ali; Faramarzi, Asaad

DOI:
10.1016/j.conbuildmat.2022.126835

Document Version
Peer reviewed version

Citation for published version (Harvard):
Dabiri, H, Kheyrodin, A & Faramarzi, A 2022, 'Predicting tensile strength of spliced and non-spliced steel bars using machine learning- and regression-based methods', *Construction and Building Materials*, vol. 325, 126835. https://doi.org/10.1016/j.conbuildmat.2022.126835

Predicting Tensile Strength of Spliced and Non-spliced Steel Bars Using Machine Learning- and Regression-based Methods

Abstract

Mechanical properties of steel reinforcement bars, which have a critical effect in the overall performance of reinforced concrete (RC) structures, should be reported and assessed before being used in structural elements. Determining bars' properties could be time-consuming and expensive specifically in the case of incorporating splices. Therefore, this study aims to predict tensile strength of bars using machine learning-based methods including nonlinear regression, ridge regression and artificial neural network. To this end, a comprehensive dataset including over 200 tests on non-spliced and spliced steel bars by mechanical couplers was collected from the available peer reviewed international publications. Bar size, splice method, steel grade, temperature and splice characteristics (length and outer diameter of couplers) were the input parameters considered for predicting tensile strength. The efficiency of the models was evaluated through Taylor diagram and common performance metrics namely coefficient of determination (R^2), root mean square error (RMSE), mean absolute error (MAE) and mean absolute percentage error (MAPE). The results demonstrated that the predicted values agreed well with the actual values reported in the experimental studies used for collecting the dataset. A parametric study was also conducted in order to examine the influence of coupler length, coupler outer diameter and temperature on the tensile strength of spliced bars. Based on the parametric study results, three different equations were suggested for calculating tensile strength of spliced bars using the mentioned parameters. The outcomes of this study can assist practitioners to effectively and accurately estimate tensile strength of spliced steel bars in reinforced concrete structures without the need to carry out expensive and timely physical tests.

Keywords: steel bars, tensile strength, machine learning, ANN, nonlinear regression, ridge regression.

1. Introduction

One of the most critical issues in reinforced concrete (RC) elements is bar splicing which could affect the overall behavior of structures under static and dynamic loads. Splicing methods introduced and investigated up to now could be categorized in three main groups: mechanical, welded and lap splices, each of which has advantages and drawbacks [1, 2].

Lap splice methods are known as the simplest splice type and could be classified as contact and non-contact [2-4]. The drawbacks of this method are: (i) bar congestion in the region of splice, (ii) being impractical for connecting existing bars and new bars, and (iii) reducing the strength or displacement capacity when they are located in the regions with inelastic deformations [5, 6].

Due to above-mentioned drawbacks, alternative splicing methods (commonly referred to mechanical bar splices) are used which could be classified into: shear-screw couplers, headed bar couplers, grouted sleeve couplers, threaded couplers and swaged couplers [7, 8]. In a mechanically spliced bar, tensile stress is transferred from one bar to the other one through the coupler and its components: in the threaded, shear screw, headed bar, swaged and grouted sleeve couplers the stress is transferred through the threads' interlock, bar surface-screws friction, male/female steel parts at the end of bars, bar's ribs and deformed sleeve friction, and the grout, respectively [9]. The benefits of incorporating mechanical methods are: fast application, being environmentally friendly, and acceptable performance. The reliable results of couplers have motivated researchers to evaluate their influence on the structures' performance [1, 7, 8, 10-14].

Tensile strength of spliced reinforcement bars should be taken into account for evaluating their performance [15]. In the grouted sleeve connections, tensile strength capacity of bars, the bond capacity between the bar and the grout, and the tensile capacity of the threaded connections (if any) are the most effective parameters for determining tensile strength of the spliced bars [16]. In the grouted head-splice sleeves the ultimate strength is slightly dependent on the ratio of head diameter to bar diameter [17]. Sleeve thickness is the other parameter which can affect the stress-strain behavior of mechanically spliced bars [18]. Based on the results of previous studies, it is proved that increasing sleeve thickness could improve confinement and bond interaction between grout and bar in a splice [18, 19]. Other significant parameters which can change the grouted-sleeve connections could be grout-sleeve bond and configuration of the splice [20]. Parametric studies have proven that increasing the sleeve length could enhance the performance of RC elements, however, the length should meet the limitations suggested by researchers [8, 21]. As far as sleeve dimensions are concerned, the diameter of sleeves should be as small as possible. Otherwise stated, the smaller the sleeve length is, the higher the tensile capacity will be. This is due to confinement increase which leads to improvement in bond strength. A range of 6-8 times of the bar diameter is also recommended for bar embedded length [22]. Several models and

equations have been proposed in experimental and numerical studies for predicting the mechanical properties of grouted sleeve connections [16, 17, 20, 23, 24].

Length, thickness and rigidity are the parameters which significantly affect the performance of other coupler types such as threaded, shear-screw and headed bar couplers. The maximum length of 15 times of the bar diameter is suggested for coupler length. Long couplers could decrease seismic parameters such as ductility or deformation capacity of RC elements. Briefly, slender and rigid couplers are not recommended to be incorporated in RC elements due to their inappropriate influence on seismic performance of structures [8, 25-27].

Splicing steel bars using welding-based methods (i.e., head-to-head, along bars and gas pressure welding) have also been investigated in several studies. According to the studies' conclusions, these types of splices could lead to satisfactory and efficient results in terms of both rebar tensile strength and seismic performance of RC elements [28-31].

In the last few decades, the application of artificial intelligence (AI) for predicting engineering parameters has been increasing because of their acceptable ability of prediction [32, 33]. In structural engineering, as an example, many studies have carried out to (i) predict mechanical properties of material like concrete and steel [34-40], (ii) predict load capacity or failure mode [31, 33, 41-46], (iii) the performance of structures under fire conditions [47-49], (iv) mechanical properties of corroded steel elements [50, 51] and (v) monitor structural health [52, 53].

Chou et al. combined a Taguchi Particle Swarm Optimization (TPSO) with a three-layer artificial neural network (ANN) to model ten mechanical components of steel bars and their relationship to quality evaluation criteria. Tensile strength and yield point of steel bars were their predicted values which agreed well with experimental values [54]. The bond strength between GFRP bars and concrete was predicted using a neuro-fuzzy inference system and ANN by Alizadeh et al. Their predicted values were compared to the values obtained by the equation available in ACI 440.1R-15 [55] and CSAS806-12 [56] and it was observed that the proposed model led to more accurate results in comparison to the values obtained by the above-mentioned equations [38]. According to the outcomes of Golafshani et al. study on predicting bond-strength of spliced bars in concrete, ANN method could be slightly more accurate than fuzzy logic (FL). Both of them, however, had appropriate and reliable prediction capacity with acceptable errors (R^2= 99.5% and 99.45% for ANN and FL, respectively) [57]. Another ANN model was also provided by Koroglu to predict the flexural bond strength of FRP bars in concrete [58]. Abdalla and Hawileh proposed a model for predicting fatigue life of steel bars. Based on the parametric study conducted in their research, stain ratio and maximum strain affect fatigue life of reinforcement bars notably [59-61].

2. Research significant

Mechanical properties of reinforcement bars should be necessarily determined for either real constructions or laboratory examinations in order to assess their quality. Tensile strength of reinforcement bars has undoubtedly a critical role in RC structural design because of its undeniable influence on the response of structures under dynamic loads. The tests carried out for this purpose (e.g., tensile strength test), however, are sometime time-consuming and costly particularly when

different types of spliced bars are used. As a result, machine learning-based methods could be a reliable solution for predicting the tensile strength of non-spliced or spliced bars.

To the knowledge of the authors, no researches have been done on determining steel bars' properties by machine learning (ML) methods so far. Hence, in the present study an attempt has been made to propose a model for predicting tensile strength of reinforcement steel bars using three ML-based models: nonlinear regression, ridge regression and ANN. Five input parameters affecting the tensile strength remarkably were considered for proposing the prediction models: bar size, splice methods, steel grade, temperature and splice characteristics including length and outer diameter of a coupler. A parametric study is also conducted in order to realize the relation between length and outer diameter of a coupler, and temperature on the tensile strength of spliced bars.

3. Collected database

For training and testing purpose of the developed ML-based framework, over 200 experimental datasets on the tensile strength of steel bars were gathered from the available literature. It is worth noting that in order to collect a high-accuracy database, internationally peer-reviewed papers and reports are selected [11, 13, 24, 62-68]. Table 1 gives information about the datasets used in this study.

Table 1. *Summary of the datasets*

Reference	*Number of tests*	*Splice method*							*Range of tensile strength (MPa)*
		Non-spliced	*Headed bar*	*Grouted*	*Shear-screw*	*Taper threaded*	*Threaded*	*Swaged*	
[11]	*3*	*1*	*0*	*0*	*0*	*0*	*2*	*0*	*602.52-643.25*
[13]	*3*	*1*	*0*	*0*	*0*	*0*	*2*	*0*	*653-674*
[24]	*12*	*12*	*0*	*0*	*0*	*0*	*0*	*0*	*569-768*
[62]	*61*	*16*	*9*	*9*	*9*	*9*	*9*	*0*	*555.72-901.14*
[63]	*24*	*6*	*0*	*0*	*0*	*0*	*18*	*0*	*480-768*
[64]	*18*	*9*	*3*	*3*	*0*	*0*	*0*	*3*	*646.04-730.84*
[65]	*4*	*2*	*0*	*0*	*2*	*0*	*0*	*0*	*520-660*
[66]	*16*	*2*	*0*	*14*	*0*	*0*	*0*	*0*	*734.29-760.49*
[67]	*2*	*2*	*0*	*0*	*0*	*0*	*0*	*0*	*655-758*
[68]	*84*	*84*	*0*	*0*	*0*	*0*	*0*	*0*	*559-889.42*
Sum.	*227*	*135*	*12*	*26*	*11*	*9*	*31*	*3*	*480-901.14*

Tensile strength of spliced or non-spliced bars could be measured by a displacement control examination according to ASTM E8 [69]. A bar is firstly marked in two pints for measuring its elongation after tensile test. Then, it is placed in the tensile test machine and incremental displacement is applied to one end of the bar until the sample fails. This process is depicted in Fig.

1. As reported in Table 1, the range of tensile strength of the collected data is 480-901.14 MPa. It should be also stated that 135 out of 227 collected datasets are non-spliced (%59) while other tests (%41) were carried out on spliced bars with different splice methods including headed bar, grouted, shear-screw, tapper threaded, threaded and swaged couplers. The mentioned methods are demonstrated in Fig. 2. It is worth explaining that although splice methods incorporated in the collected database are not the same, they all meet the required criteria of the design Codes (e.g., ACI318-19 [70] and UBC1997 [71]) regarding mechanical splice methods: spliced bars, should provide $1.25f_y$ of a non-spliced bar in tension and compression. The splice technique is not specified by the Codes and the mentioned provision should be considered for any type of mechanical splice.

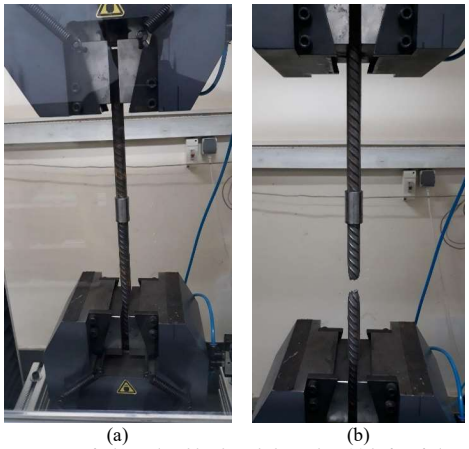

(a) (b)

Figure 1*. Tensile test setup of a bar spliced by threaded coupler: (a) before failure, (b) after failure*

Commented [AF(E1]: Add citations and references for these figures

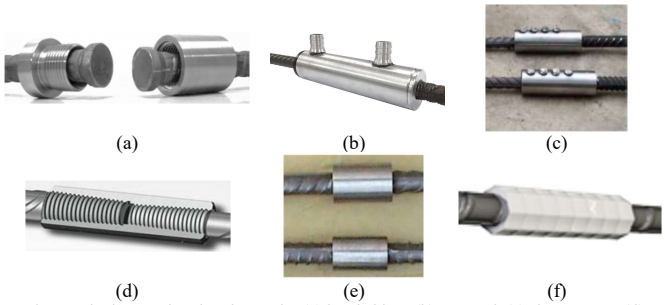

(a) (b) (c)

(d) (e) (f)

Figure 2*. Different splice methods considered in this study: (a) headed bar, (b) Grouted, (c) shear-screw, (d) Taper threaded, (e) threaded and (f) Swaged couplers.*

Commented [AF(E2]: same as above

As noted before, various factors could affect tensile strength of steel bars. In this study, the parameters which have the highest impact are considered as input variables. In order to consider the influence of coupler dimensions in the prediction models, their length and outer diameter are used as two input variables in the ML-based models. Temperature is also claimed to be a significantly effective parameter on tensile strength of steel bars [63]. Six different temperatures were considered in the collected dataset for testing steel bars: 20°, 25°, 100°, 300°, 400° and 500° C. A series of bar sizes in the range of 12-32 mm (bar diameter) were taken into consideration in the dataset. The reason of choosing the mentioned sizes is that they are known as the most common sizes utilized in construction. It has been tried to include both spliced and non-spliced type for each bar size in the selected database. Seven different steel grades were also considered as the sixth input parameter: ASTM 615 grade 60, ASTM 615 grade 75, D500E, HBR400, HBR500, S400 and S500. Overall, the collected test samples are different in terms of coupler type, coupler length, coupler outer diameter, bar diameter, steel grade and temperature, and they all have met the Codes requirement regarding mechanical splice methods (providing $1.25f_y$ of non-spliced bar in tension and compression).

Table 2 summarizes the above-mentioned explanations regarding the database by providing statistical parameters including minimum, maximum, mean, variance and standard deviation. The distribution of the parameters considered as input are also depicted in Fig. 3.

***Table 2**. Statistical properties of the input and output parameters used for the prediction model.*

	Min.	*Max.*	*Mean*	*Variance*	*STD*
Bar size (mm)	*12.00*	*32.00*	*24.21*	*54.49*	*7.38*
Coupler length (mm)	*40*	*490.54*	*88.07*	*20096.70*	*141.76*
Coupler outer diameter (mm)	*7.29*	*64.00*	*17.60*	*535.80*	*23.15*
Temperature	*20.00*	*500.00*	*46.28*	*7429.56*	*86.19*
Tensile strength (MPa)	*480.00*	*901.14*	*692.35*	*7255.71*	*85.18*

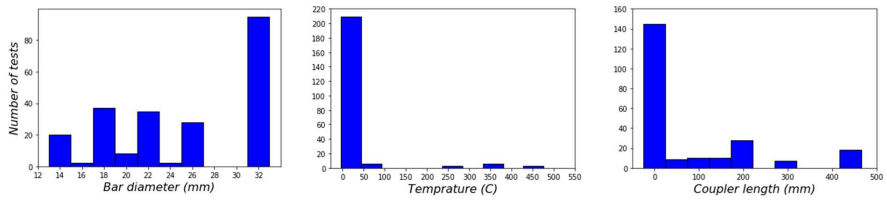

(a) (b) (c)

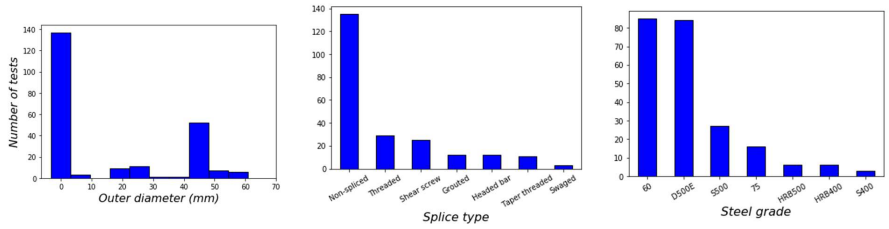

(d) (e) (d)

Figure 3. *Distribution of the input parameters: (a)bar diameter, (b) temperature, (c) coupler length, (d) outer diameter of coupler, (e) splice type and (f) steel grade.*

In order to figure out the correlations between input and output parameters, the Pearson correlation matrix is provided in Table 3. It should be mentioned that Pearson correlation coefficient is the covariance of the two variables divided by the product of their standard deviations. Large coefficients show higher linear correlation between two variables, while low coefficients stand for either less linear correlation or independency of them. As expected, steel grade (0.63) and bar size (0.60) are the most effective parameters while splicing method (0.08) has the lowest influence on the output. Coupler characteristics are also effective parameters on tensile strength with correlation of about 0.3.

Table 3. *Correlation matrix of the variable parameters*

		Input variables						*Output*
		Splice method	*Steel grade*	*Bar size (mm)*	*Coupler length (mm)*	*Coupler outer diameter (mm)*	*Temperature (℃)*	*Tensile strength (MPa)*
Input variables	*Splice method*	*1.00*						
	Steel grade	*-0.31*	*1.00*					
	Bar size (mm)	*0.13*	*-0.66*	*1.00*				
	Coupler length (mm)	*0.59*	*-0.54*	*0.35*	*1.00*			
	Coupler outer diameter (mm)	*0.75*	*-0.63*	*0.38*	*0.81*	*1.00*		
	Temperature (℃)	*0.25*	*0.25*	*-0.19*	*0.00*	*0.02*	*1.00*	
Output	***Tensile strength (MPa)***	***0.08***	***0.63***	***0.60***	***0.28***	***0.36***	***-0.35***	***1.00***

4. ML-based models

In order to propose a model for predicting tensile strength of spliced and non-spliced steel bars ML- and regression-based methods are used: nonlinear regression, ridge regression and ANN. These methods are explained in this section.

4.1. Nonlinear regression

Regression methods are mainly classified as linear and nonlinear analysis. Nonlinear regression is known as a very popular method utilized in mathematics, science and engineering since it provides more reliable and valid predictions in comparison to linear regression [72, 73]. The most notable strength of this method is its capacity which allows researchers to select the fixed and adjustable parameters [74].

In nonlinear regression, data are modeled by a function, $f(x; \theta)$, which is a nonlinear combination of parameters:

$$y = f(x; \theta) + \varepsilon \qquad (1)$$

Where $y \in \mathbb{R}$ is the response variable, $x \in \mathbb{R}^k$ are variables and $\theta \in \mathbb{R}^p$ are parameters and ε refers to error with zero mean and variance σ^2. When the regression function, f, is nonlinear in Θ, the statistical inferential is known as nonlinear regression analysis [72].

4.2. Ridge regression

Predicting the coefficients of a model in linear regression, which uses least square fit method, relies on the independence of the model parameters. When there are correlations between parameters the least square estimate will be sensible to random errors in the output. This issue could be due to a small training dataset. One of the possible addresses for this problem could be ridge regression method which reduces the sensitivity of the output to the training dataset by considering a small value of bias [75-77].

The classical way for minimizing the squared loss is the ordinary least square method given in Eq. 2:

$$\sum_i (y_i - \beta_i x_i)^2 \qquad (2)$$

Ridge regression, however, minimizes the cost given in Eq. (3):

$$J(\beta) = \sum_i (y_i - \beta^T x_i)^2 + \frac{||\beta||^2}{\rho} \qquad (3)$$

Where x_i and y_i are training datasets, β is the variance of the estimate and $||.||$ is the Euclidean norm of a vector. The ridge regression decreases the estimate variance by introducing the regression parameters, ρ, which controls the trade-of between the bias and estimate variance [77].

4.3. ANN

Artificial neural networks (ANN) method is a data driven supervised machine learning model which has attracted researchers' attention because of its abilities to simplify and increase the accuracy of complicated systems with large inputs. The performance of ANN is inspired by simplified functioning of the human brain [52, 78].

The architecture of the neural networks depends heavily on the complexity of the problem. However, they are typically formed by four main parts: (i) input layer: the number of neurons in

this layer are equal to the number of variables in input data, (ii) hidden layers: which are considered to update weights of the signals obtained from input layer, (iii) output layer: which is the target parameter which should be predicted and (iv) a bias: which could be connected to hidden and output neurons. The mathematical description of an ANN is given in Eq. (4) [38, 52, 57, 78]:

$$O_j = f\sum\left(w_{ij}I_i + b\right) \qquad (4)$$

Where O_j is the model output, w_{ij} is associated weight which is updated in each epoch, I_i is input data and b is bias. It should be taken into consideration that the hidden layer and the output neuron could be processed by feeding in into an activation function, f. A typical architecture of the ANN is schematically illustrated in Fig. 4.

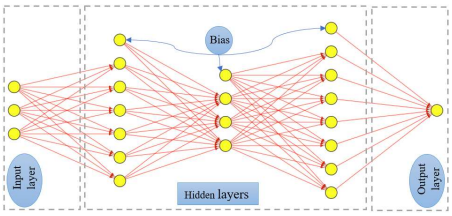

Figure 4. *Typical architecture of an artificial neural network.*

Minimizing the error during training process is one of the most significant parts of ANN models which is done by updating the weights, w_{ij}. One of the most effective approaches which can be used for minimizing the errors is gradient decent with quick performance in minimizing [59]. It should be also stated that desirable accuracy of an ANN method is obtained by trial-and-error process to achieve the most appropriate architecture [40, 43].

5. Models

In order to achieve an appropriate prediction model with an acceptable level of accuracy the model properties (e.g., number of input layers, number of hidden layers, number of neurons, etc.) should be optimized. Although several suggestions regarding the model optimization have been made, none of them warranty a high-accurate model. Therefore, trial-and-error process are used to find out the model architecture with satisfactory results.

R^2 coefficient was evaluated to find the most accurate ANN model. It should be mentioned that higher R^2 reflects the better match between predicted and actual values. Fig. 5 shows the number of epochs versus MSE which was used for finding the best number of irritations.

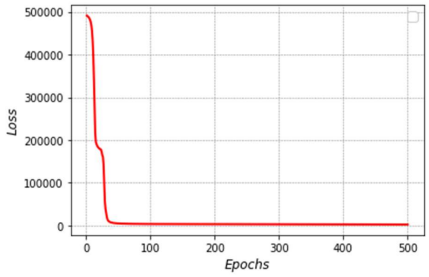

***Figure 5**. Optimization cost in terms of MSE*

After several trial-and-error process, it was realized that an ANN model with six input layers, four hidden layers with 19, 17, 15, 15 neurons in the first to fourth layers, respectively and one output layer could lead to reliable prediction values. The Rectified linear unit (ReLu) function, as provided in Eq. (5), is used in the proposed ANN method. This function usually results in better performance and generalization compared to the other activation function. The final architecture of the ANN model is depicted in Fig. 6.

$$f(x) = \max(0, x) = \begin{cases} x_i \; if \; x_i > 0 \\ 0 \; if \; x_i < 0 \end{cases} \qquad (5)$$

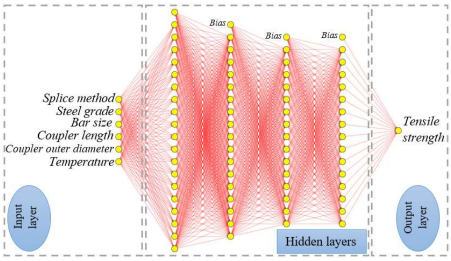

***Figure 6.** Architecture of the final ANN model proposed in this study.*

As far as training and testing datasets are concerned, 85% of the datasets was selected for training while 15% was used for testing the model reliability in all the ML-based methods. It is noteworthy that training and testing divisions were made randomly in order to prevent any man-selection effect on training process.

6. Results

The output of the proposed ML-based models for predicting tensile strength of steel bars is presented in this section. The correlations between predicted and actual values for training and testing divisions of the databases are shown respectively in Fig. 7 (a) and (b). The fit line is also illustrated. A comparison between each predicted data with the corresponding actual data is also made in Fig. 7 (c), (d) for training and testing data, respectively.

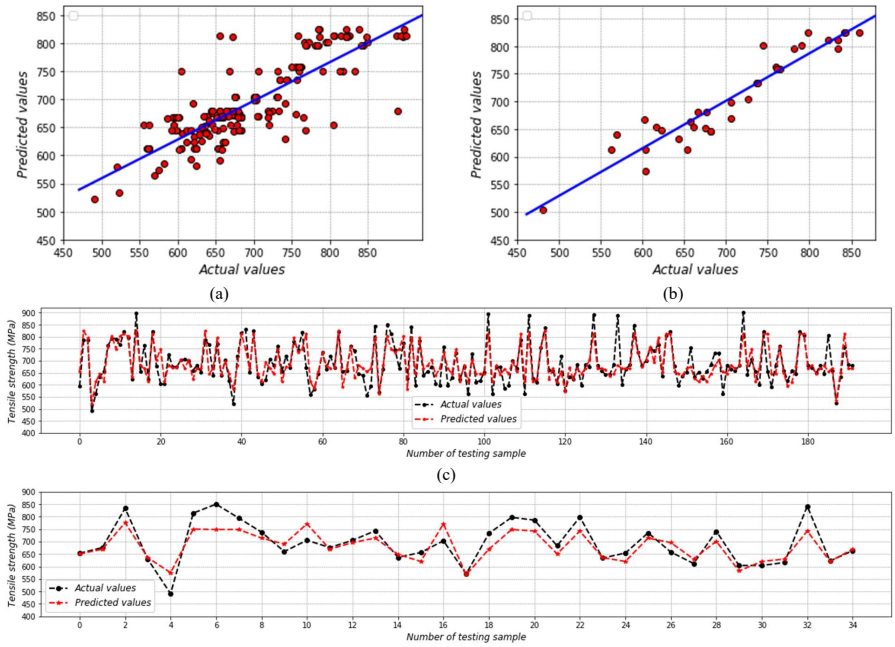

Figure 7*. Predicted and actual values of the nonlinear regression model: (a) correlation of training datasets, (b) correlation of testing datasets, (c) comparison for training datasets and (d) comparison of testing datasets.*

The predicted values by ridge regression and ANN models are also presented and compared graphically in Fig. 8 and Fig. 9, respectively.

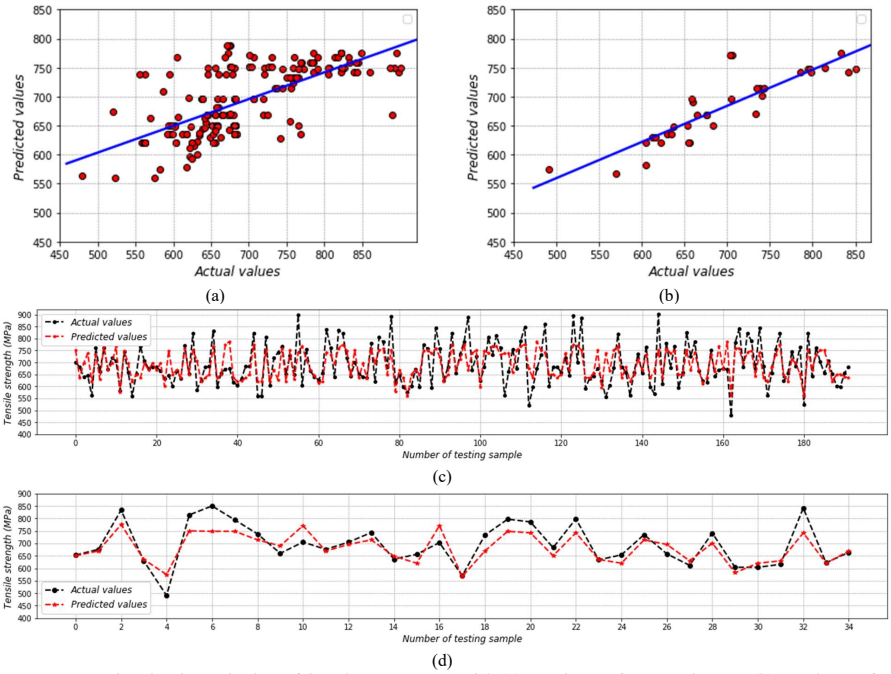

Figure 8. *Predicted and actual values of the ridge regression model: (a) correlation of training datasets, (b) correlation of testing datasets, (c) comparison for training datasets and (d) comparison of testing datasets.*

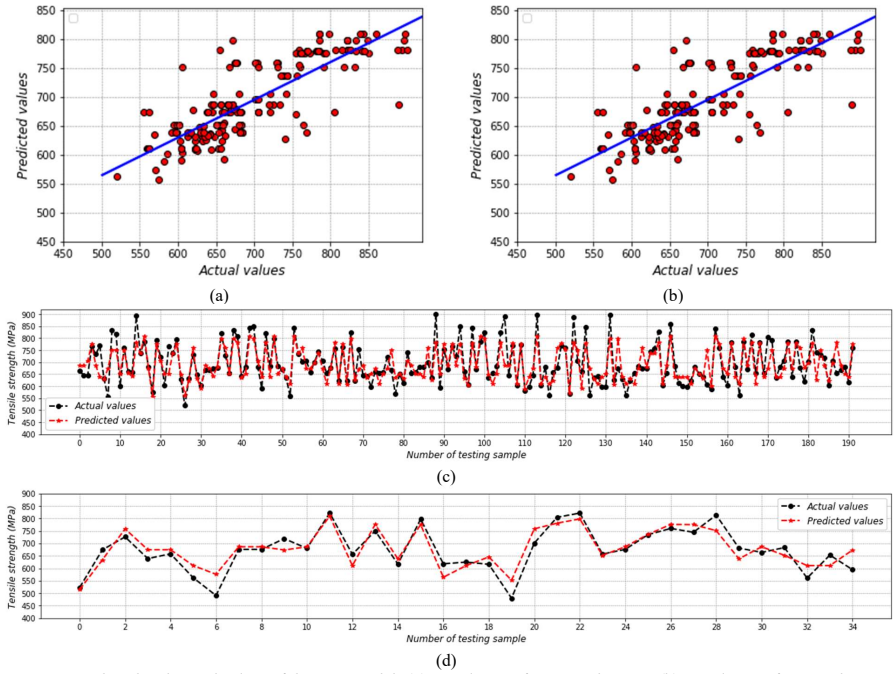

Figure 9. *Predicted and actual values of the ANN model: (a) correlation of training datasets, (b) correlation of testing datasets, (c) comparison for training datasets and (d) comparison of testing datasets.*

The close match between predicted and actual values for the training datasets depicted in figures 7(c), 8(c) and 9(c) proves that nonlinear regression, ridge regression and ANN methods have the capacity to learn the relationships between input variable and output parameter for predicting tensile strength of sliced and non-spliced steel bars.

According to the comparisons of testing datasets made and presented in Fig. 7(d), Fig. 8(d) and Fig. 9(d), it could be also claimed that the predicted values obtained by all the three ML- and regression-based methods match well with the actual values. The nonlinear regression model, however, has a higher accuracy compared to other models. The quantitative difference between the models' accuracy is provided in the next section.

7. Models' assessment and discussions

In order to evaluate the accuracy of predicted values obtained by the ML- and regression-based models in this study, the outcomes are discussed in terms of four performance metrics given in Eq. (6-9) [35, 57]:

$$RMSE = \left(\frac{1}{n}\sum_{i=1}^{n}(\hat{y}_i - y_i)^2\right)^{0.5} \qquad (6)$$

$$MAE = \frac{1}{n}\sum_{i=1}^{n}|\hat{y}_i - y_i| \quad (7)$$

$$MAPE = \frac{1}{n}\sum_{i=1}^{n}\left|\frac{\hat{y}_i - y_i}{y_i}\right| \quad (8)$$

$$R^2 = 1 - \frac{\sum_i(\hat{y}_i - y_i)^2}{\sum_i(y_i - \bar{y}_i)^2} \quad (9)$$

RMSE, MAE, MAPE and R^2 refers to root mean square error, mean absolute error, mean absolute percentage error and coefficient of determination, respectively. y is the actual output, $\hat{y}$ is the predicted output, n is the number of data records and $\bar{y}$ is the mean of the dataset. The above-mentioned metrics are obtained and provided in Table 4.

Table 4. *Performance metrics of the proposed prediction models.*

Model	*RMSE (MPa)*	*MAE (MPa)*	*MAPE (-)*	*R^2 (-)*
Nonlinear regression	*29.63*	*23.5*	*3.51*	*0.90*
Ridge regression	*44.12*	*34.47*	*4.81*	*0.72*
ANN	*38.76*	*32.35*	*5.09*	*0.81*

Taking the data presented in Table 4 into account, it could be claimed that the values predicted by all the three models match well with the actual values reported in the experimental tests. Nevertheless, the nonlinear regression model showed the highest R^2 coefficient (90%) which shows the highest accuracy in comparison to other methods. RMSE, MAE and MAPE coefficients of the nonlinear model are also lower than those obtained by other models. By comparing the ridge regression model with the ANN model, it could be said that the results of the ANN are more reliable.

In order to assess the accuracy of the proposed models more precisely, they are compared through Taylor diagram as displayed in Fig. 10. It is worth mentioning that Taylor diagram is a well-known diagram widely used for evaluating and comparing the prediction models. The real and predicted values are positioned in a coordination system by considering standard deviation (vertical and horizontal axis), RMSE (circular lines) and correlation coefficient (radial lines). The closer to the real value a model is positioned, the more accurate it will be. As could be obviously seen in Fig. 10, the nonlinear model with RMSE=29.63, R^2=0.90 and standard deviation=83.25 is the closest model to the real values (red star) and therefore is introduced as the most accurate method for predicting tensile strength of spliced and non-spliced bars. The ANN model with RMSE, R^2 and standard deviation of respectively 38.76, 0.81 and 75.25 is positioned between NL and Ridge models. The Ridge model, on the other hand, is the farthest model to the real values in comparison to other proposed models (RMSE=44.12, R^2=0.72 and standard deviation=58.46).

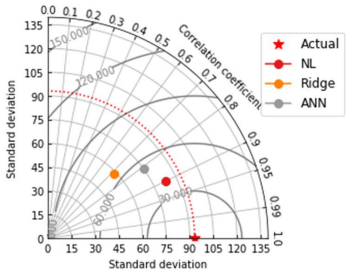

***Figure 10**. Comparing the proposed models by Taylor Diagram*

8. Parametric investigation

The most accurate prediction model introduced in the previous section is used to figure out the influence of significant parameters -namely coupler length (l_c), Coupler outer diameter (OD_c) and temperature- on the tensile strength of spliced bars. To this aim, the results of a tensile test on a 16 mm-diameter bar spliced by a threaded coupler is chosen from the literature [63]. Then, the above-mentioned parameters are varied as below to generate a database:

- Coupler length: 50-250 mm by the step of 20 mm (samples 2-12 in Table 5)
- Coupler outer diameter: 10-31 mm by the step of 3 mm (samples 13-20 in Table 5)
- Temperature: 20-660 °C by the step of 80 °C (samples 21-29 in Table 5)

It should be explained that the range of the parameters is carefully defined based on the values reported in the relevant literature. The tensile strength value predicted by the proposed nonlinear model for each generated sample is reported in Table 5. The variation of tensile strength of spliced bars is also depicted graphically in Fig. 11.

Table 5. *Tensile strength of a spliced bar with different coupler length, coupler outer diameter and temperature*

Sample No.	*Coupler length (mm)*	*Outer diameter (mm)*	*Temperature*	*Ultimate strength (MPa)*
*1**	*206*	*25*	*20*	*612*
2	*50*	*25*	*20*	*643.63*
3	*70*	*25*	*20*	*651.56*
4	*90*	*25*	*20*	*656.4*
5	*110*	*25*	*20*	*658.15*
6	*130*	*25*	*20*	*656.8*
7	*150*	*25*	*20*	*652.36*
8	*170*	*25*	*20*	*644.83*
9	*190*	*25*	*20*	*634.2*
10	*210*	*25*	*20*	*620.48*
11	*230*	*25*	*20*	*603.67*
12	*250*	*25*	*20*	*583.77*
13	*206*	*10*	*20*	*633.04*
14	*206*	*13*	*20*	*630.39*
15	*206*	*16*	*20*	*628.10*
16	*206*	*19*	*20*	*626.19*
17	*206*	*22*	*20*	*624.65*
18	*206*	*25*	*20*	*623.47*
19	*206*	*28*	*20*	*622.67*
20	*206*	*31*	*20*	*622.24*
21	*206*	*25*	*20*	*623.47*
22	*206*	*25*	*100*	*636.52*
23	*206*	*25*	*180*	*637.00*
24	*206*	*25*	*260*	*624.91*
25	*206*	*25*	*340*	*600.26*
26	*206*	*25*	*420*	*563.04*
27	*206*	*25*	*500*	*513.26*
28	*206*	*25*	*580*	*450.91*
29	*206*	*25*	*660*	*375.99*

**The sample taken from the literature [63].*

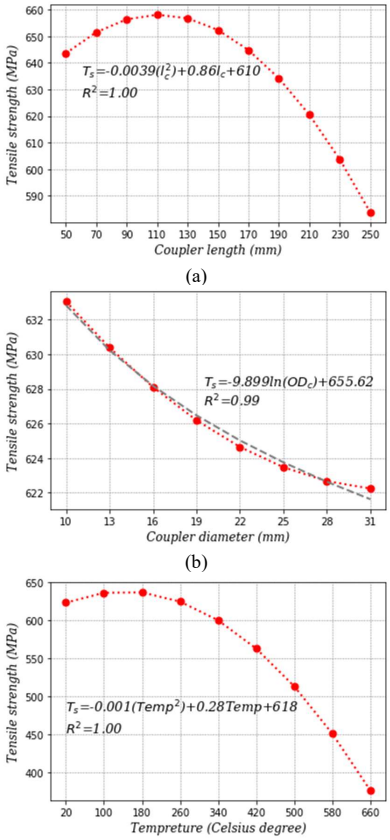

Figure 11*. The variation of tensile strength of a 16 mm-diameter bar spliced by coupler by changing (a) coupler length, (b) coupler outer diameter and (c) temperature.*

8.1. Coupler length (l_c)

Taking Fig. 11a into account, it could be understood that increasing coupler length up to specific value (here 110 mm), increases tensile strength of a spliced bar. Then, increasing coupler length might lead to reduction in bars' tensile strength. Similar experimental studies have also reported the same results. Several researchers [8, 25, 26, 79] have claimed that long couplers might result in reduction in ductility and deformation capacity, earlier failure, and concrete-rebar slip.

The fitting curve shown in Fig. 11a is used to drive Eq. 10 which expresses the relationship between coupler length (l_c, mm) and tensile strength (T_S, MPa):

$$T_s = -0.0039{l_c}^2 + 0.86l_c + 610 \qquad (10)$$

8.2. Coupler outer diameter (OD_c)

As could be clearly observed in Fig. 11b, outer diameter of a coupler (OD_c) affects tensile strength conversely. Otherwise stated, by increasing OD_c, tensile strength decreases. This might be due to the change in coupler's rigidity which affects spliced bars' performance remarkably. As also concluded in experimental investigations, rigid couplers reduce ductility and therefore are not recommended to be used for splicing bars [8, 26].

According to the diagram demonstrated in Fig. 11b, the logarithmic relationship between outer diameter of a coupler (OD_c, mm) and tensile strength (MPa) is obtained and give in Eq. 11:

$$T_s = -9.899 ln OD_c + 655.62 \qquad (11)$$

8.3. Temperature

The curve illustrated in Fig. 11c reveals that increasing temperature up to 180°C, increases tensile strength of a spliced bar. Higher temperature, however, could reduce tensile strength notably. These results are in line with the similar experimental studies carried out to investigate the influence of temperature on couplers' performance [63]. The relationship between tensile strength and temperature (Temp, °C) could be suggested as Eq. 12:

$$T_s = -0.001 Temp^2 + 0.28 Temp + 618 \qquad (12)$$

9. Summary and conclusions

In the present study, an attempt was made to predict the tensile strength of spliced and non-spliced steel bars. To this aim, three prediction models were proposed using ML- and regression-based methods: nonlinear regression, ridge regression and ANN. A dataset containing over 200 samples collected from peer-reviewed publications were divided into training and testing parts randomly. The most effective parameters including bar size, splice methods, splice length, splice outer diameter, temperature and steel grade were considered as input variables for predicting tensile strength of steel bars (output). The outcomes were assessed and compared by Taylor diagram and performance metrics including R^2, MAE, RMSE and MAPE. A parametric study was also conducted and equations were provided for predicting tensile strength of spliced bars.

Taking the study results into account, it could be concluded that:

- All of the three models showed an acceptable level of accuracy, however, the prediction model proposed using nonlinear regression method led to more reliable results in comparison to ridge regression and ANN methods.
- Moreover, it could be claimed that simple, quick and inexpensive ML- and regression-based methods could be introduced as a reliable alternative technique for time-consuming and expensive experimental tests carried out to determine tensile strength of spliced and non-spliced steel bars.
- According to the results of the parametric investigation, increasing coupler length and temperature (up to 110 mm and 180°C, respectively) increased tensile strength of a 16 mm-diameter bar spliced by a coupler. Longer length and higher temperature, reduced tensile strength significantly. Furthermore, increasing outer diameter of couplers reduced tensile strength which might be because of the rigidity increase of the coupler.

- It should be stated that this study aimed at predicting tensile strength of spliced and non-spliced steel bars. Further studies are undoubtedly required in order to predict other significant parameters of steel bars (e.g., yield strength, yield strain, ultimate strain) which exhibit the performance of splice methods and affect the structures' response remarkably. More importantly, other ML-based methods (e.g., Random Forest, Support Vector Machine) are recommended to be used and compared for predicting mechanical properties of steel bars.

References

1. Kheyroddin, A. and H. Dabiri. *Cyclic performance of RC beam-column joints with mechanical or forging (GPW) splices; an experimental study*. in *Structures*. 2020. Elsevier.
2. Najafgholipour, M., et al. *The performance of lap splices in RC beams under inelastic reversed cyclic loading*. in *Structures*. 2018. Elsevier.
3. Alyousef, R., T. Topper, and A. Al-Mayah, *Crack growth modeling of tension lap spliced reinforced concrete beams strengthened with fibre reinforced polymer wrapping under fatigue loading.* Construction and Building Materials, 2018. **166**: p. 345-355.
4. Metelli, G., J. Cairns, and G. Plizzari, *The influence of percentage of bars lapped on performance of splices.* Materials and Structures, 2015. **48**(9): p. 2983-2996.
5. Tarquini, D., J.P. de Almeida, and K. Beyer, *Experimental investigation on the deformation capacity of lap splices under cyclic loading.* Bulletin of Earthquake Engineering, 2019. **17**(12): p. 6645-6670.
6. Alias, A., et al., *Performance of grouted splice sleeve connector under tensile load.* Journal of Mechanical Engineering and Sciences (JMES), 2014. **7**: p. 1096-1102.
7. Dahal, P.K. and M. Tazarv, *Mechanical bar splices for incorporation in plastic hinge regions of RC members.* Construction and Building Materials, 2020. **258**: p. 120308.
8. Tazarv, M. and M.S. Saiidi, *Seismic design of bridge columns incorporating mechanical bar splices in plastic hinge regions.* Engineering Structures, 2016. **124**: p. 507-520.
9. Dabiri, H., A. Kheyroddin, and A. Dall'Asta, *Splice methods used for reinforcement steel bars: A state-of-the-art review.* Construction and Building Materials, 2022. **320**: p. 126198.
10. Zheng, Y., et al., *Parametric study on a novel grouted rolling pipe splice for precast concrete construction.* Construction and Building Materials, 2018. **166**: p. 452-463.
11. Kheyroddin, A., et al. *Experimental investigation of using mechanical splices on the cyclic performance of RC columns*. in *Structures*. 2020. Elsevier.
12. Bompa, D. and A. Elghazouli. *Ductility considerations for mechanical reinforcement couplers*. in *Structures*. 2017. Elsevier.
13. Bompa, D. and A. Elghazouli, *Inelastic cyclic behaviour of RC members incorporating threaded reinforcement couplers.* Engineering Structures, 2019. **180**: p. 468-483.
14. Wu, S., et al., *Seismic performance of a novel partial precast RC shear wall with reserved cast-in-place base and wall edges.* Soil Dynamics and Earthquake Engineering, 2022. **152**: p. 107038.
15. Zeng, X., et al., *Dynamic tensile behavior of steel HRB500E reinforcing bar at low, medium, and high strain rates.* Materials, 2020. **13**(1): p. 185.

16. Yuan, H., et al., *Tensile behavior of half grouted sleeve connections: Experimental study and analytical modeling.* Construction and Building Materials, 2017. **152**: p. 96-104.
17. Seo, S.-Y., B.-R. Nam, and S.-K. Kim, *Tensile strength of the grout-filled head-splice-sleeve.* Construction and Building Materials, 2016. **124**: p. 155-166.
18. Lin, F. and P. Zhao, *Behavior of Grouted Sleeve Splice for Steel Profile under Tensile Loadings.* Materials, 2020. **13**(9): p. 2037.
19. Kim, H.-K., *Bond strength of mortar-filled steel pipe splices reflecting confining effect.* Journal of Asian Architecture and Building Engineering, 2012. **11**(1): p. 125-132.
20. Ling, J.H., A.B.A. Rahman, and I.S. Ibrahim, *Feasibility study of grouted splice connector under tensile load.* Construction and Building Materials, 2014. **50**: p. 530-539.
21. Sayadi, A.A., et al., *The relationship between interlocking mechanism and bond strength in elastic and inelastic segment of splice sleeve.* Construction and Building Materials, 2014. **55**: p. 227-237.
22. Ling, J.H., et al., *Tensile capacity of grouted splice sleeves.* Engineering Structures, 2016. **111**: p. 285-296.
23. Zhang, W., et al., *Tensile behavior of half grouted sleeve connection at elevated temperatures.* Construction and Building Materials, 2018. **176**: p. 259-270.
24. Lin, F. and X. Wu, *Mechanical performance and stress–strain relationships for grouted splices under tensile and cyclic loadings.* International Journal of Concrete Structures and Materials, 2016. **10**(4): p. 435-450.
25. Han, W., et al., *Seismic behavior of precast columns with large-spacing and high-strength longitudinal rebars spliced by epoxy mortar-filled threaded couplers.* Engineering Structures, 2018. **176**: p. 349-360.
26. Bompa, D. and A. Elghazouli. *Monotonic and cyclic performance of threaded reinforcement splices*. in *Structures*. 2018. Elsevier.
27. Haber, Z.B., M.S. Saiidi, and D.H. Sanders, *Seismic performance of precast columns with mechanically spliced column-footing connections.* ACI Structural Journal, 2014. **111**(3): p. 639-650.
28. Dabiri, H. and A. Kheyroddin. *An experimental comparison of RC beam-column joints incorporating different splice methods in the beam*. in *Structures*. 2021. Elsevier.
29. Kheyroddin, A., S. Rouhi, and H. Dabiri, *An experimental study on the influence of incorporating lap or forging (GPW) splices on the cyclic performance of RC columns.* Engineering Structures, 2021. **241**: p. 112434.
30. Issa, C.A. and A. Nasr, *An experimental study of welded splices of reinforcing bars.* Building and environment, 2006. **41**(10): p. 1394-1405.
31. Alwanas, A.A.H., et al., *Load-carrying capacity and mode failure simulation of beam-column joint connection: Application of self-tuning machine learning model.* Engineering Structures, 2019. **194**: p. 220-229.
32. Kim, S.-E., et al., *Comparison of machine learning algorithms for regression and classification of ultimate load-carrying capacity of steel frames.* Steel and Composite Structures, 2020. **37**(2): p. 193-209.
33. Ahmadi, M., et al., *New empirical approach for determining nominal shear capacity of steel fiber reinforced concrete beams.* Construction and Building Materials, 2020. **234**: p. 117293.

34. Hawileh, R.A., et al., *Models for predicting elastic modulus and tensile strength of carbon, basalt and hybrid carbon-basalt FRP laminates at elevated temperatures.* Construction and building materials, 2016. **114**: p. 364-373.
35. Behnood, A. and E.M. Golafshani, *Machine learning study of the mechanical properties of concretes containing waste foundry sand.* Construction and Building Materials, 2020. **243**: p. 118152.
36. Shariati, M., et al., *A novel hybrid extreme learning machine–grey wolf optimizer (ELM-GWO) model to predict compressive strength of concrete with partial replacements for cement.* Engineering with Computers, 2020: p. 1-23.
37. Kandiri, A., E.M. Golafshani, and A. Behnood, *Estimation of the compressive strength of concretes containing ground granulated blast furnace slag using hybridized multi-objective ANN and salp swarm algorithm.* Construction and Building Materials, 2020. **248**: p. 118676.
38. Alizadeh, F., H. Naderpour, and M. Mirrashid, *Bond strength prediction of the composite rebars in concrete using innovative bio-inspired models.* Engineering Reports, 2020. **2**(11): p. e12260.
39. Naderpour, H., et al., *Innovative models for prediction of compressive strength of FRP-confined circular reinforced concrete columns using soft computing methods.* Composite Structures, 2019. **215**: p. 69-84.
40. Latif, S.D., *Concrete compressive strength prediction modeling utilizing deep learning long short-term memory algorithm for a sustainable environment.* Environmental Science and Pollution Research, 2021: p. 1-9.
41. Abuodeh, O.R., J.A. Abdalla, and R.A. Hawileh, *Prediction of shear strength and behavior of RC beams strengthened with externally bonded FRP sheets using machine learning techniques.* Composite Structures, 2020. **234**: p. 111698.
42. Vu, Q.-V., V.-H. Truong, and H.-T. Thai, *Machine learning-based prediction of CFST columns using gradient tree boosting algorithm.* Composite Structures, 2021. **259**: p. 113505.
43. Esfandiari, M. and G. Urgessa. *Progressive collapse design of reinforced concrete frames using structural optimization and machine learning*. in *Structures*. 2020. Elsevier.
44. Mirrashid, M. and H. Naderpour, *Innovative Computational Intelligence-Based Model for Vulnerability Assessment of RC Frames Subject to Seismic Sequence.* Journal of Structural Engineering, 2021. **147**(3): p. 04020350.
45. Mangalathu, S., S.-H. Hwang, and J.-S. Jeon, *Failure mode and effects analysis of RC members based on machine-learning-based SHapley Additive exPlanations (SHAP) approach.* Engineering Structures, 2020. **219**: p. 110927.
46. Moradi, M.J., et al., *Prediction of the load-bearing behavior of SPSW with rectangular opening by RBF network.* Applied Sciences, 2020. **10**(3): p. 1185.
47. Naser, M. and H. Zhou, *Machine Learning to Derive Unified Material Models for Steel Under Fire Conditions*, in *Intelligent Data Analytics for Decision-Support Systems in Hazard Mitigation*. 2021, Springer. p. 213-225.
48. Naser, M., *Mechanistically informed machine learning and artificial intelligence in fire engineering and sciences.* Fire Technology, 2021: p. 1-44.
49. Naser, M., et al., *StructuresNet and FireNet: Benchmarking databases and machine learning algorithms in structural and fire engineering domains.* Journal of Building Engineering, 2021. **44**: p. 102977.

50. Chun, P.-j., et al., *Evaluation of tensile performance of steel members by analysis of corroded steel surface using deep learning.* Metals, 2019. **9**(12): p. 1259.
51. Karina, C., P.-j. Chun, and K. Okubo, *Tensile strength prediction of corroded steel plates by using machine learning approach.* Steel Compos. Struct, 2017. **24**(5): p. 635-641.
52. Mishra, M., *Machine learning techniques for structural health monitoring of heritage buildings: A state-of-the-art review and case studies.* Journal of Cultural Heritage, 2020.
53. Sun, H., H.V. Burton, and H. Huang, *Machine learning applications for building structural design and performance assessment: state-of-the-art review.* Journal of Building Engineering, 2020: p. 101816.
54. Chou, P.-Y., J.-T. Tsai, and J.-H. Chou, *Modeling and optimizing tensile strength and yield point on a steel bar using an artificial neural network with taguchi particle swarm optimizer.* IEEE access, 2016. **4**: p. 585-593.
55. ACI, *Guide for the Design and Construction of Structural Concrete Reinforced with FRP Bars (ACI 440.1 R-15)*. 2015: Farmington Hills, MI: (ACI) American Concrete Institute.
56. CSA, *Design and Construction of Building Structures with Fibre-Reinforced Polymers*. 2012, Canadian Standards Association: Ontario, Canada.
57. Golafshani, E.M., et al., *Prediction of bond strength of spliced steel bars in concrete using artificial neural network and fuzzy logic.* Construction and building materials, 2012. **36**: p. 411-418.
58. Köroğlu, M.A., *Artificial neural network for predicting the flexural bond strength of FRP bars in concrete.* Science and Engineering of Composite Materials, 2019. **26**(1): p. 12-29.
59. Abdalla, J.A. and R.A. Hawileh, *Artificial neural network predictions of fatigue life of steel bars based on hysteretic energy.* Journal of computing in civil engineering, 2013. **27**(5): p. 489-496.
60. Abdalla, J.A. and R. Hawileh, *Modeling and simulation of low-cycle fatigue life of steel reinforcing bars using artificial neural network.* Journal of the Franklin Institute, 2011. **348**(7): p. 1393-1403.
61. Abdalla, J., et al., *Energy-based prediction of low-cycle fatigue life of BS 460B and BS B500B steel bars.* Materials & Design, 2009. **30**(10): p. 4405-4413.
62. Rowell, S.P., et al., *High strain-rate testing of mechanical couplers*. 2009, Engineer research and development center Vicksburg MS geotechnical
63. Bompa, D. and A. Elghazouli, *Elevated temperature characteristics of steel reinforcement incorporating threaded mechanical couplers.* Fire Safety Journal, 2019. **104**: p. 8-21.
64. Jordan, E.J., *Experimental Studies of Reinforcing Steel and Shape Memory Alloys in Mechanically Spliced Connections for Seismic Application*. 2018.
65. Chidambaram, R.S. and P. Agarwal, *Performance evaluation of innovative hybrid rebar coupler in reinforced concrete beams subjected to monotonic loading.* Structural Concrete, 2018. **19**(3): p. 892-903.
66. Lloyd, W., *Qualification of the bar-lock rebar coupler for use in nuclear safety-related applications mechanical testing program and performance analysis.* Idaho National Engineering and Environmental Laboratory Materials Department, Report No. INEEL/EXT-02-01387, 2001.
67. Higgins, C.C., et al., *Seismic Retrofits for Square Reinforced Concrete Columns Using Titanium Alloy Bars*. 2020: School of Civil and Construction Engineering, Oregon State University.

68. Housing, D.o.B.a., *Report on Grade 500E Steel Reinforcement*. 2005: Wellington, New Zealand.
69. ASTM, E., *16a Standard Test Methods for Tension Testing of Metallic Materials*. 2018, ASTM International: West Conshohocken.
70. 318-19, A., *Building Code Requirement for Structural Concrete and Commentary*. 2019, American Concrete Institute Committee.
71. UBC-97, *Uniform Building Code* 1997, International Council of Building Officials: USA.
72. Huang, H.-H. and S.-Y. Huang, *Nonlinear regression analysis.* International Encyclopedia of Education, 2010: p. 339-346.
73. Orchinik, M. and T.F. Murray, *Steroid hormone binding to membrane receptors*, in *Methods in Neurosciences*. 1994, Elsevier. p. 96-115.
74. Parsons, Z.D. and K.S. Gates, *Redox regulation of protein tyrosine phosphatases: methods for kinetic analysis of covalent enzyme inactivation.* Methods in enzymology, 2013. **528**: p. 129-154.
75. Xiaohong, D., et al., *Statistical estimation the thermal conductivity of MWCNTs-SiO2/Water-EG nanofluid using the ridge regression method.* Physica A: Statistical Mechanics and its Applications, 2020. **537**: p. 122782.
76. Moreno-Salinas, D., et al., *Modelling of a surface marine vehicle with kernel ridge regression confidence machine.* Applied Soft Computing, 2019. **76**: p. 237-250.
77. Yan, C., et al., *An artificial bee colony-based kernel ridge regression for automobile insurance fraud identification.* Neurocomputing, 2020. **393**: p. 115-125.
78. Roshani, M.M., et al., *Predicting the Effect of Fly Ash on Concrete's Mechanical Properties by ANN.* Sustainability, 2021. **13**(3): p. 1469.
79. Karabinis, A.I., *Reinforced concrete beam-column joints with lap splices under cyclic loading.* Structural Engineering and Mechanics, 2002. **14**(6): p. 649-660.